THE ASTROPHYSICAL JOURNAL, 311:345–359, 1986 December 1

DUST GRAINS AND GAS IN THE CIRCUMSTELLAR ENVELOPES AROUND LUMINOUS RED GIANT STARS

B. ZUCKERMAN
University of California Los Angeles
AND
H. M. DYCK
University of Hawaii
Received 1986 February 21; accepted 1986 May 20

ABSTRACT

With 12, 25, 60, and 100 μm fluxes given in the *IRAS* Point Source Catalog, we have constructed color-color plots that include more than 100 infrared bright red-giant stars. Carbon-rich and oxygen-rich red giants can be distinguished from each other based on the ratio of their 25 to 60 μm fluxes, but not by the two other flux ratios, 12 to 25 μm and 60 to 100 μm. We interpret this to indicate that the dust grain emissivity index p between 25 and 60 μm is larger, on average, for O-rich giants by approximately 0.4 where p is defined by: emissivity $\propto \nu^p$. Over the frequency range 12 to 100 μm the mean value of p for C-rich stars is about 1.1 and is slightly larger for O-rich stars.

In two previous papers, we reported CO rotational emission from 64 cool red giants with large fluxes in the *IRAS* Point Source Catalog. In the present paper we report CO emission from an additional 15 stars as well as HCN emission toward 11 stars. We use these HCN data and the color-color plots described above, in conjunction with a reexamination of the *IRAS* low-resolution spectrometer (LRS) data, to classify and reclassify various stars as oxygen- or carbon-rich. For example, we classify FX Ser, IRC +60144, AFGL 2102, and AFGL 2151, all of which are classified as O-rich in the Revised AFGL Catalog, as C-rich. We suggest that AFGL 2343 is probably an unusual oxygen-rich supergiant located far from the galactic plane. Five objects that we observed show strong narrow CO or HCN emission, and we identify these as young stars embedded in molecular clouds.

In 1985 June the carbon star V Hya displayed a narrow CO emission feature superposed on a standard broad stellar CO profile. The narrow emission, which was not present in 1976 June, probably represents the first example of a CO maser ever seen in either a circumstellar or interstellar environment.

Subject headings: infrared: sources — interstellar: grains — stars: carbon — stars: circumstellar shells — stars: late-type

I. INTRODUCTION

The *IRAS*[1] Point Source Catalog and the Revised Air Force Geophysics Laboratory Catalog (RAFGL, Price and Murdock 1983) are rich sources of broad-band infrared data on luminous red-giant stars with large mass-loss rates. In two previous papers (Zuckerman and Dyck 1986; Zuckerman, Dyck, and Claussen 1986; hereafter Papers I and II), we described CO $J = 1 \rightarrow 0$ and/or $J = 2 \rightarrow 1$ emission from 64 stars with large 12 and/or 25 μm fluxes in the *IRAS* catalog. Combining these data with previous CO data on 50 additional infrared luminous stars from Knapp and Morris (1985), we investigated radiation pressure driven mass loss (Paper I) and massive carbon-rich stars near the galactic plane (Paper II). In the present paper we extend these previous results in various ways.

1) We have detected, for the first time, CO emission from an additional 15 stars, including AFGL 2343, a possible runaway supergiant located far from the galactic plane and, perhaps, NGC 6302, an unusual planetary nebula. In addition, we obtained a high signal-to-noise $J = 1 \rightarrow 0$ CO spectrum of V Hya, a classical N-type carbon star first seen in CO emission in 1976 June. The current (1985 June) spectrum displayed a narrow emission feature which may be a circumstellar CO maser.

2) We detected $J = 1 \rightarrow 0$ HCN emission toward 11 stars. Most of these are located near the galactic plane where contamination by interstellar CO emission often makes measurement of the circumstellar CO profile difficult or impossible. The HCN data are consistent with and strengthen the main conclusion of Paper II: carbon-rich red-giant stars with large outflow velocities that are located near the galactic plane are, almost certainly, included among the most massive carbon stars in the Galaxy. In addition, the HCN data can be used, sometimes in conjunction with *IRAS* data (see below), to clarify and correct the classification of certain stars.

3) Because the approximately 130 stars with CO or HCN emission are among the brightest and reddest giant stars in the *IRAS* Point Source Catalog, they are an optimum sample to use to investigate systematic regularities that might be present in the broad-band flux distributions. Hacking *et al.* (1985) constructed an *IRAS* color-color diagram (12/25 μm versus 25/60 μm) for a somewhat different sample of stars and noticed that oxygen-rich and carbon-rich stars lie in different regions of the diagram. They basically did not interpret this effect except to suggest weakly that carbon stars are surrounded by more cool dust than are O-rich stars. Because our sample is essentially

[1] This research was supported (in part) under NASA's *IRAS* Data Analysis Program and funded through the Jet Propulsion Laboratory.

the brightest giant stars in the *IRAS* catalog, we are able to investigate the 60/100 μm flux ratios in addition to the 12/25 and 25/60 μm fluxes. Our interpretation of the color-color plots differs from that of Hacking *et al.* (1985), viz., between 25 and 60 μm, the dust grain emissivity index p (where emissivity $\propto \nu^p$) is larger, on the average, in the O-rich stars by approximately 0.4, indicating a significant difference in the properties of the grains in carbon- and in oxygen-rich environments. The effect is *not* due to more cool dust near the carbon-rich stars.

4) We have used microwave spectral data (e.g., OH and H_2O maser emission and CO and HCN "thermal" emission), location in the color-color plots described in (3) above, and *IRAS* low-resolution spectrometer (LRS) data, to establish more reliable classifications for many stars listed in the *IRAS* and RAFGL catalogs.

The structure of the paper is as follows. First, we describe the CO and HCN observations. Second, we discuss the color-color plots and use them to derive values for p for both O-rich and C-rich stars between 12 and 100 μm. Third, we consider various interesting individual stars emphasizing, in many cases, their classifications in terms of C/O abundance ratios. We defer discussion of mass-loss rates of gas and of dust grains until a later paper.

II. EQUIPMENT AND OBSERVATIONS

We used the 12 m telescope of the National Radio Astronomy Observatory[2] equipped with a dual polarization cooled mixer receiver. Data were obtained in 1985 early June and early November for the $J = 1 \rightarrow 0$ transitions of CO and HCN, respectively. At the 115.2712 GHz CO transition frequency, the double sideband temperatures of the two receivers were measured by the NRAO staff to be 170 K. We measured the full half-power beamwidth to be 52″ in elevation. At the 88.63185 GHz HCN transition frequency, the DSB temperatures of the two receivers were measured by the NRAO staff to be 200 K. We measured the elevation HPBW to be 69″.

The spectral line "back end" consisted of 256 channel filter banks; the width of an individual channel was 1 MHz for CO observations and either 500 kHz or 1 MHz for HCN observations. The data were obtained by switching the telescope between a star and a reference position (typically 5′ or 10′ away in azimuth) at a rate of 1/60 Hz and subtracting the off-source spectra from the on-source spectra. Total integration times, including time spent at the reference position, varied between one-half hr and three hr for all stars listed in Tables 1 and 2 that have not been detected previously in CO or HCN emission. Some stars that have been detected previously in CO and/or HCN are included in Tables 1 and 2 so as to facilitate comparison of our data with those of other observers.

As described in Paper I, our target list consisted of sources in the *IRAS* Point Source Catalog that have fluxes greater than 100 Jy at 12 μm or greater than 50 Jy at 25 μm. Four objects that we detected in CO emission and one detected in HCN emission appear to be young stars embedded in molecular clouds. Those are listed in Table 3 and described in § IV*c* below. Data for the other newly detected stars, all apparently red giants, are summarized in Tables 1 and 2. The listed 1950

[2] The National Radio Astronomy Observatory is operated by Associated Universities, Inc., under contract with the National Science Foundation.

TABLE 1

CO $J = 1 \rightarrow 0$ EMISSION TOWARD EVOLVED STARS[a]

Object (1)	RAFGL (2)	α_{1950} (3)	δ_{1950} (4)	Position Reference (5)	Spectral Type (6)	T_B(K) (7)	V_{LSR} (km s^{-1}) (8)	V_∞ (km s^{-1}) (9)	Remarks (10)
R Scl	215	$1^h24^m40^s.0$	−32°48′07″	1	C(SR)	0.70	−18.4	17.5	Previously detected
IRC +60144	595	4 30 45.9	62 10 12	2	C	0.34	−46.2	14.5	Previously detected
IRAS 0807−3615		8 07 28.1	−36 15 35	3	C	0.20	11.8	17.3	
	5250	8 17 06.9	−21 34 47	3	C	0.15	−9.3	15.8	$J = 2 \rightarrow 1$ Previously detected (Paper I)
	5254	9 11 40.9	−24 38 54	4	C	0.66	0.1	13.4	
IRC +10216	1381	9 45 14.8	13 30 41	5	C(M)	9.1	−25.9	15.9	Previously detected
CIT 6	1403	10 13 11.0	30 49 17	5	C(SR)	1.9	−1.5	16.3	Previously detected
V Hya	1439	10 49 11.3	−20 59 05	1	C(SR)	0.56[b]	−15.6[b]	14.2[b]	See Fig. 5
RT Vir	1594	13 00 05.7	5 27 15	1	M(SR)	0.15	16.8	8.4	
IRAS 1610−4205		16 10 34.9	−42 05 29	3	M	0.42	−82.2	14.0	
NGC 6302		17 10 21.3	−37 02 43	6	O-rich	0.28	−46.4	16.4	See Fig. 6
	6815S	17 15 04.6	−32 24 15	3	M	0.11	26.4	25.1	
	5379	17 41 07.4	−31 54 24	3	M?	0.47	−20.5	20.5	Data are for $J = 2 \rightarrow 1$, *not* for $J = 1 \rightarrow 0$
	5416	17 53 24.0	−30 30 25	3	C?	0.24[c]	−18.4	31.8	Near galactic center Interstellar? (see § II)
IRC +20370	2232	18 39 41.7	17 38 16	7	C	0.77	0.4	15.6	Previously detected
IRC −30398	2289	18 56 02.9	−29 54 29	2	M	0.30	−6.8	13.2	
RS CrA	5552	18 59 34.5	−39 47 22	3	M	0.26	17.4	20.7	
V3880 Sgr	2330	19 05 55.0	−22 19 09	2	M	0.09	23.5	22.2	
	2343	19 11 25.0	0 02 18	3	G	0.21	105.0	33.9	Supergiant? (see Fig. 7)
	2362	19 16 08.0	23 43 53	8	M	0.12	23.9	20.0	
SV Peg	2845	22 03 31.0	35 06 17	1	M(SR)	0.11	6.2	11.0	
CU Cep	2865	22 09 45.1	56 47 27	2	M(M)	0.09	−41.5	7.4	Interstellar? (see § II)
	2999	22 55 39.5	58 33 28	9	M	0.23[c]	−58.4	17.6	
TX Psc	3147	23 43 40.1	3 12 34	1	C	0.16	10.0	10.6	See note (d)

[a] Except for AFGL 5379, where the tabulated data apply to the $J = 2 \rightarrow 1$ transition.
[b] Tabulated CO data apply only to the broad kinematic component.
[c] Narrow CO emission also present at a velocity near V_{LSR}.
[d] Also detected by Ericksson *et al.* 1986.

REFERENCES.—(1) SAO Catalog; (2) Kleinmann and Joyce positions given in *IRAS* catalog; (3) *IRAS* Point Source Catalog; (4) See § II of Paper I; (5) Kleinmann and Payne-Gaposchkin 1979; (6) Rodriguez *et al.* 1985; (7) Zuckerman *et al.* 1977; (8) Joyce *et al.* 1977; (9) Gehrz and Hackwell 1976.

TABLE 2

HCN $J = 1 \rightarrow 0$ Emission toward Evolved Stars

Object (1)	RAFGL (2)	α_{1950} (3)	δ_{1950} (4)	Position Reference (5)	T_B(K) (6)	V_{LSR} (km s^{-1}) (7)	V_∞ (km s^{-1})[a] (8)	Remarks (9)
	67	$0^h24^m47^s.0$	69°22′16″	1	0.057	−25.2	16.6	
	190	1 14 26.3	66 58 08	2	0.07	−36.2	14.9	
	482	3 18 38.8	70 16 27	3	0.06	−9.7	10.8	V_∞ poorly determined
IRC +60144	595	4 30 45.9	62 10 12	4	0.07	−44.7	19.9	See Fig. 4
IRAS 0530+3029		5 30 32.0	30 29 03	5	<0.08			
	809	5 40 33.3	32 40 49	1	0.13	−30.1	22.7	
Y Tau	5168	5 42 40.7	20 40 33	6	$\lesssim$0.12	~6		Possible line
	865	6 01 17.5	7 26 03	7	0.084	45.3	15.4	
	971	6 34 16.5	3 28 05	3	<0.05			
	5250	8 17 06.9	−21 34 47	5	0.052	−2.8	15.4	
IRC +10216	1381	9 45 14.8	13 30 41	8	5.0	−22.0	16.0	Previously detected
CIT 6	1403	10 13 11.0	30 49 17	8	0.4	2.5	17.1	Previously detected
R CrB	4219	15 46 30.7	28 18 32	9	<0.04			Hydrogen-deficient
	5146S	17 48 16.7	−28 24 52	5	<0.04			
	2023	17 51 13.9	−25 49 00	3	0.062	6.5	10.0	See § IV*a*
					0.03	114.6	16.3	Probable line
FX Ser	2067	18 04 04.8	−9 41 42	4	<0.06			
	2178	18 28 52.4	−8 37 27	3	<0.04			
IRC +10401	2310	19 00 52.9	7 26 15	10	0.27	21.6	28.0	See Fig. 3
	2333	19 07 34.0	9 21 56	5	0.08	47.6	19.0	
RY Sgr	5559	19 13 16.9	−33 36 41	9	<0.04			Hydrogen-deficient
	2494	19 59 24.8	40 47 18	3	<0.08			
IRAS 2002+3910		20 02 48.0	39 10 03	5	<0.1			
	2513	20 07 15.0	31 16 52	3	0.036	19.4	22.0	
V1549 Cyg	2074	21 03 32.6	51 36 18	4	<0.03			
IRAS 2128+5050		21 28 15.0	50 50 43	5	<0.07			

[a] V_∞ not corrected for HCN hyperfine pattern (see § IV*a*).

References.—(1) Lebofsky *et al.* 1978; (2) Gehrz and Hackwell 1976; (3) Joyce *et al.* 1977; (4) Kleinmann and Joyce positions given in *IRAS* catalog; (5) *IRAS* Point Source Catalog; (6) RAFGL Catalog and *IRAS* Point Source Catalog; (7) Low *et al.* 1976; (8) Kleinmann and Payne-Gaposchkin 1979; (9) SAO Catalog; (10) RAFGL Catalog, Zuckerman *et al.* 1977, and Kleinmann and Joyce (see ref. [4]).

epoch positions are usually of high quality, except for a few *IRAS* positions. In Table 1 column (6) gives the spectral type of the central star. Here C and M indicate stars that we believe to be carbon-rich (C/O > 1) or oxygen-rich (C/O < 1), respectively. Justification for some of these classifications may be found in § IV*b*. The letters SR and M contained in parentheses indicate semiregular and Mira-type variable stars, respectively.

The columns headed T_B give the peak brightness temperature averaged over the main beam of the telescope and corrected for all telescope and atmospheric losses; that is, T_B is the Rayleigh-Jeans equivalent brightness temperature that would be measured by a perfect antenna above Earth's atmosphere. We estimate that errors in T_B are approximately 20% for the stronger sources (dominated by systematic errors) and perhaps twice as large for weaker sources with poor signal-to-noise ratios.

The columns headed V_{LSR} and V_∞ give the central velocity of the CO or HCN profile with respect to the local standard of rest and the terminal outflow velocity, respectively. V_∞ is basically one-half the width of the profile at zero power. Both V_{LSR} and V_∞ were determined, in almost all cases, by fitting profiles of the form given in either equation (2) in Knapp and Morris (1985) or equation (7) in Morris (1985). Most of the line shapes resemble parabolas or rectangles, although some of the narrower ones can be fitted rather well by Gaussians. We estimate that errors in V_{LSR} are typically 1 km s^{-1} and, in V_∞, 2 km s^{-1} (but occasionally, perhaps, a good deal larger for V_∞). For HCN, V_{LSR} is based on the rest frequency of the strongest hyperfine component, 88.63185 GHz (see, also, § IV*a*).

In a few cases we obtained spectra near but not on the target star to ensure that the observed line was really associated with the star and was not interstellar. AFGL 5416 (see Table 1) lies within 3° of the galactic center. Since many interstellar clouds with large internal velocity dispersions are known to be in this general direction, it is conceivable that the broad feature indicated in Table 1 for AFGL 5416 is really interstellar. (We were

TABLE 3

Pre-Main-Sequence Stars in Molecular Clouds

Object (1)	α_{1950} (2)	δ_{1950} (3)	T_B(K) (4)	V_{LSR} (km s^{-1}) (5)	D (kpc) (6)	L_* ($L_\odot$) (7)	Remarks (8)
RAFGL 5124	$4^h32^m28^s.7$	51°06′39″	1.6	−36.4	5	5×10^4	HCN data
RAFGL 5206	6 41 12.5	−1 05 02	2.4	49.4	6	7×10^4	
RAFGL 5502	18 30 50.8	−5 03 27	23.1	42.4	3	2×10^4	Near kinematic distance
IRAS 2155+5907	21 55 49.1	59 07 33	5.1	−90.0	10	1×10^5	
IRAS 2214+5206	22 14 14.7	52 06 26	8.3	−37.4	4	1×10^4	

Note.—All positions are from the *IRAS* Point Source Catalog.

switching the telescope by 5′ in azimuth and there was not time to map the CO source.) Indeed, when we searched, in 1986 April, for the $J = 2 \rightarrow 1$ CO transition toward AFGL 5416, the line that was detected at -18 km s^{-1} had a smaller brightness temperature than the $1 \rightarrow 0$ line. Thus, we suspect that the $1 \rightarrow 0$ line may well be interstellar. We also observed CU Cep in 1986 April and detected a very narrow $J = 2 \rightarrow 1$ line near -41 km s^{-1}. The narrowness of both the $1 \rightarrow 0$ (Table 1) and $2 \rightarrow 1$ lines and the location of CU Cep in the galactic plane is suggestive of interstellar, rather than circumstellar, CO. The line toward NGC 6302 may also be interstellar (see § IV*b*).

III. DUST GRAIN EMISSIVITY

A quantity of considerable interest in circumstellar and interstellar studies is the opacity (cross section per gram of material) of dust grains as a function of wavelength which we denote as $k(\lambda)$. Knowledge of k at a specific wavelength is crucial if one desires to derive the mass of dust implied by a given flux of far-infrared radiation at that wavelength. If, in addition, one can deduce $k(\lambda)$ over a wide range of λ, then one may learn more about the physical properties of the dust grains in individual sources (see Sopka *et al.* 1985, and references therein for more details). The opacity $k(\lambda)$ can be written in terms of a dimensionless emission efficiency, Q: $k(\lambda) = 3Q(\lambda)/4a\rho$, where a and ρ are the radius and density of a typical grain. In the absence of significant band structure (e.g., the silicate feature in O-rich stars or the SiC and related features in carbon stars), Q can be written to a good approximation in terms of p, the emissivity index, as $Q(\lambda) \propto \lambda^{-p}$. This form has a significant computational advantage and allows us to discuss gross properties of the emitting dust.

One method for deducing p is to analyze the shape of the far-infrared thermal continua in various stars. Using equation (3) in Sopka *et al.* (1985), we can write the ratio of the observed flux, $F(\lambda)$, at two wavelengths, λ_1 and λ_2, as

$$\frac{F(\lambda_1)}{F(\lambda_2)} = \frac{Q(\lambda_1)}{Q(\lambda_2)} \frac{\xi(\lambda_1)}{\xi(\lambda_2)} . \tag{1}$$

Here ξ, defined in equation (4) in Sopka *et al.* (1985), is a convolution of the spatially distributed Planck function, $B(\lambda, T)$, with the telescope beam pattern $P(r, \theta)$. Following the prescription given in Appendix A of Sopka *et al.* (1985), we have evaluated ξ at the four *IRAS* wavelengths as a function of p and an assumed distance to a given star. Specifically, we have assumed that the entire envelope is optically thin to the photospheric radiation in which case $T(r) \propto r^{-2/(4+p)}$. Here $T(r)$ is the dust grain temperature as a function of radial distance from the central star. This expression ignores the steepening of $T(r)$ in the inner, optically thick region of the envelope. At the longer *IRAS* wavelengths this region contains only a small percentage of the emitting mass of the envelope (see, e.g., Appendix A in Sopka *et al.* 1985). At 12 and 25 μm the effect of the steepening of $T(r)$ on $\xi(\lambda)$ can be more substantial, but, even here, its importance is mitigated since we are interested only in the *ratio* $\xi(12\ \mu\text{m})/\xi(25\ \mu\text{m})$. For $P(r, \theta)$ we use approximations to the *IRAS* beam patterns which are given in the last two columns of Table II C.3 of the *IRAS* Catalogs and Atlases Explanatory Supplement. For most of the stars plotted in Figures 1 and 2, the *IRAS* beam is much larger than the size of region that emits the preponderance of the emission at each *IRAS* wavelength. Therefore, the calculated values for ξ are rather insensitive to the exact form assumed for $P(r, \theta)$.

The flux ratios, $F(\lambda_1)/F(\lambda_2)$, may be obtained from the *IRAS* Point Source Catalog, and we have plotted data for 136 stars in Figure 1 and for somewhat fewer stars in Figure 2. (Reliable 100 μm *IRAS* fluxes are not always available.) The 136 stars include all stars known to us for which CO and/or HCN rotational emission have been detected and for which reasonably reliable *IRAS* fluxes exist, at least at 12, 25, and 60 μm. Included among the 136 plotted stars are six from Table 2 of Paper I for which neither CO nor HCN have been detected yet. The location of these six stars in Figures 1 and 2 appear quite normal (compared to stars with detectable CO emission), except that the two symbiotic stars, 83 and 84, appear to have unusually small 60 μm fluxes relative to their 25 μm fluxes.

It is clear from Figure 1 that the 60 μm/25 μm flux ratio is larger, typically, in carbon-rich stars than it is in oxygen-rich stars.

Hacking *et al.* (1985) have constructed a similar version of our Figure 1—their Figure 1—from a somewhat different set of red-giant stars. They tentatively suggested that the enhanced 60 μm fluxes in the C-rich stars, relative to the O-rich stars, are evidence for larger amounts of cool dust at large distances from the C-rich sample. We disagree with this interpretation of the *IRAS* data for the following reasons.

We have taken advantage of the fact that our sample of stars is sufficiently bright at far-infrared wavelengths to construct a color-color plot, Figure 2, utilizing the 100 μm *IRAS* fluxes. As may be seen from Table 1 in Hacking *et al.* (1985), this is not possible for their (fainter) set of stars. If enhanced 60 μm fluxes were, in fact, due to large amounts of cool dust surrounding the C-rich stars, then we might expect them to display enhanced 100 μm fluxes as well. There is no evidence of this in Figure 2.

Stars with relatively large values of $F(25)/F(12)$ and $F(60)/F(25)$ lie in the upper right-hand quadrants of Figures 1*a* and 1*b*. These stars have either large mass-loss rates relative to stars in the left-hand half of Figure 1*a*, or mass-loss rates which have decreased with time or both; that is, these are precisely those stars that are surrounded by large amounts of cool dust. Note that even in this subset of the total sample of stars, the C-rich stars in Figure 1*a* lie systematically above the O-rich stars indicating smaller values of p for the former sample. (For a more detailed discussion of the characteristic far-infrared flux distributions of stars with large mass-loss rates, see Sopka *et al.* [1985] and with mass-loss rates decreasing with time, see Zuckerman and Lo [1986].)

In summary, we interpret Figures 1 and 2 to indicate a systematic difference in the value of p for C-rich and O-rich stars between 25 and 60 μm, but no obvious difference in p between the two types of stars from 12 to 25 μm and from 60 to 100 μm.

In their investigation of the spectra of carbon stars in the 15–40 μm spectral range, Forrest, Houck, and McCarthy (1981) found evidence for an emission band near 25 μm. More recently, Goebel and Moseley (1985) obtained data which defined the long-wavelength limit of the emission band to lie near 50 or 60 μm. They also found that the band is present in the spectrum of only some carbon stars. We compared the spectral ranges of the 25 and 60 μm *IRAS* bands and the emission band, and we conclude that the latter will usually have little or no effect on the observed ratio $F(60)/F(25)$ (in comparison to the values that this ratio would have obtained in the absence of any band structure). If any systematic effect exists, it appears that correcting for the observed emission band could make the difference in the gross (i.e., broad-band)

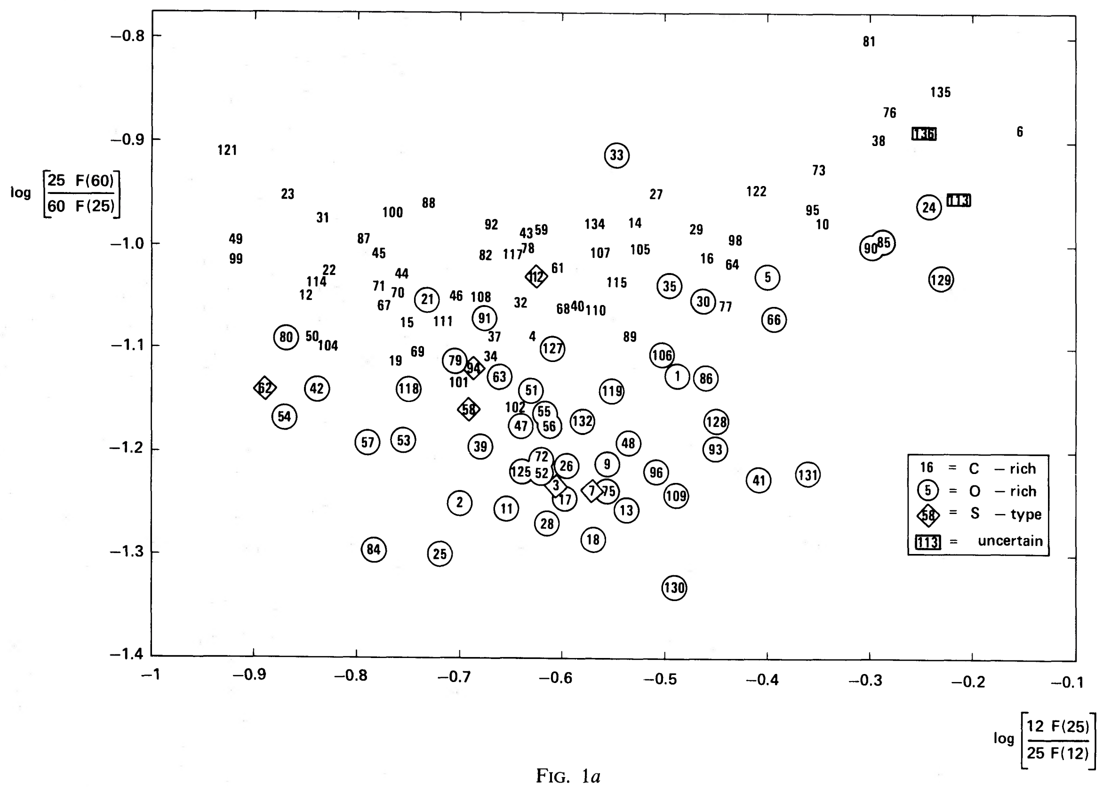

FIG. 1a

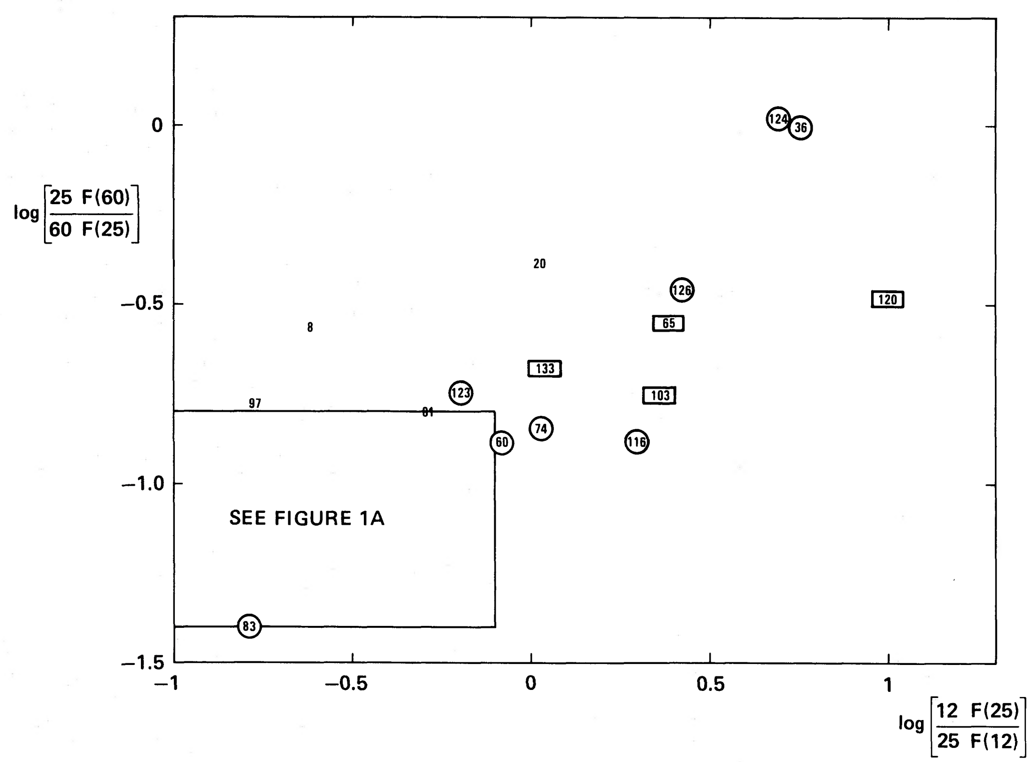

FIG. 1b

FIG. 1.—Color-color plot of *IRAS* fluxes (F) at 12, 25, and 60 μm. Fig. 1a is an expanded portion of Fig. 1b. The significance of the different symbols is given in the lower right-hand corner of Fig. 1a. See also the caption to Fig. 2; The number key is printed with Fig. 2. The fluxes used to construct Figs. 1 and 2 are those quoted in the Point Source Catalog. They have not been color corrected.

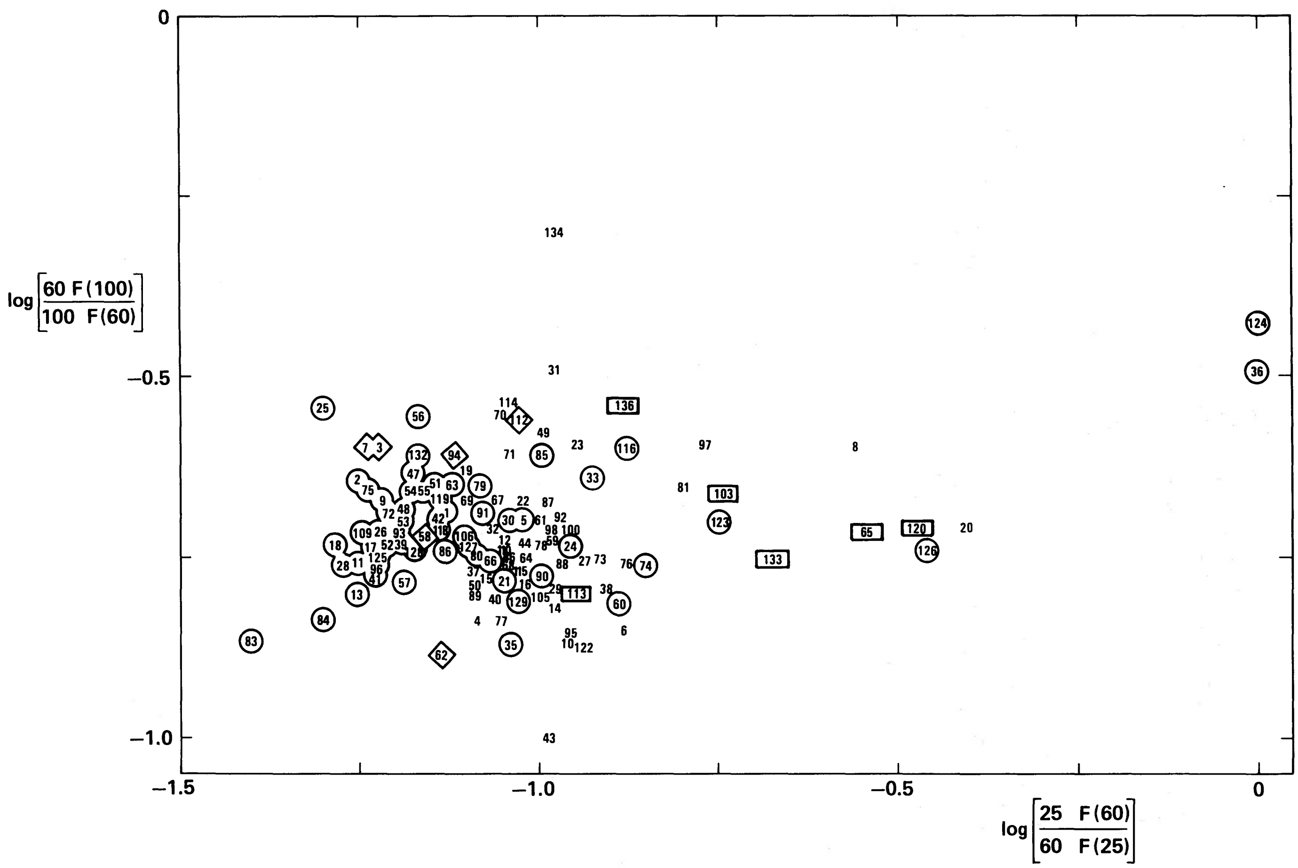

FIG. 2.—Color-color plot of *IRAS* fluxes (F) at 25, 60, and 100 μm. See Fig. 1 for the significance of the different symbols. According to the *IRAS* Point Source Catalog, there may be problems with the quality of the flux measurement and/or the correlation of the *IRAS* source with the point source template for the following stars: at 60 μm, stars 45 and 48; at 100 μm, stars 22, 31, 32, 33, 70, 115, and 116.

1) IRC +40004
2) T Cas
3) R And
4) AFGL 67
5) IRC +10011
6) AFGL 190
7) S Cas
8) R Scl
9) IRC +50049
10) *IRAS* 0215+2822
11) Mira
12) R For
13) IRC −30023
14) AFGL 482
15) IRC +50096
16) AFGL 5102
17) NML Tau
18) V Eri
19) IRC +60144
20) AFGL 618
21) IRC +60150
22) R Lep
23) W Ori
24) IRC +50137
25) R Aur
26) IRC +60154
27) AFGL 809
28) IRC +70066
29) AFGL 865
30) IRC +60169
31) UU Aur
32) AFGL 971
33) GX Mon
34) AFGL 1085
35) VY CMa
36) OH 231.8+4.2
37) AFGL 1235
38) AFGL 5250
39) RS Cnc
40) AFGL 5254
41) IW Hya
42) R Leo
43) IRC +10216
44) CIT 6
45) U Hya
46) V Hya
47) R Crt
48) AFGL 4136
49) Y CVn
50) RU Vir
51) RT Vir
52) SW Vir
53) R Hya
54) W Hya
55) RX Boo
56) X Her
57) 30 Her
58) W Aql
59) IRC −10502
60) IRC +10420
61) V1129 Cyg
62) χ Cyg
63) RR Aql
64) AFGL 2494
65) *IRAS* 2002+3910
66) IRC −10529
67) V Cyg
68) AFGL 2686
69) IRC +00499
70) IRC +40485
71) S Cep
72) EP Aqr
73) *IRAS* 2148+5301
74) *IRAS* 2155+6204
75) TW Peg
76) AFGL 3068
77) AFGL 3099
78) IRC +40540
79) R Cas
80) α Her
81) Red Rectangle
82) R CrB
83) CH Cyg
84) R Aqr
85) PZ Cas
86) IRC +20326
87) T Dra
88) AFGL 2135
89) ADGL 2155
90) AFGL 2199
91) IRC +10365
92) IRC +20370
93) IRC +30021
94) W And
95) AFGL 341
96) CIT 4
97) U Cam
98) *IRAS* 0453+4427
99) S Aur
100) Y Tau
101) AFGL 935
102) AFGL 954
103) *IRAS* 0713+1005
104) V CrB
105) AFGL 1922
106) MW Her
107) AFGL 2154
108) IRC +00365
109) IRC +10374
110) AFGL 2259
111) IRC +10401
112) R Cyg
113) *IRAS* 2131+5631
114) PQ Cep
115) AFGL 2901
116) *IRAS* 2227+5435
117) AFGL 3011
118) α Ori
119) GY Aql
120) AFGL 2343
121) TX Psc
122) *IRAS* 0807−3615
123) *IRAS* 1610−4205
124) NGC 6302
125) RS CrA
126) AFGL 6815S
127) AFGL 2289
128) AFGL 2330
129) AFGL 2362
130) CU Cep
131) AFGL 2999
132) SV Peg
133) AFGL 5379
134) AFGL 2513
135) AFGL 2333
136) AFGL 5416

25 to 60 μm emissivity indices between C-rich and O-rich stars even more pronounced than we calculate.

With equation (1) and flux ratios from Figures 1 and 2, we may calculate values of p between 12 and 100 μm. To calculate ξ and thence p for an individual star requires knowledge of the distance, d, to the star (see, e.g., Sopka *et al.* [1985], eq. [8]). In a future paper (Sopka, Dyck, and Zuckerman 1986), we will evaluate ξ for each star in Figure 1 using the best available estimate for d. Here we evaluate ξ by assuming a single representative distance (approximately 800 pc) for all stars in Figure 1 since we are concerned only with the average value of p for O-rich and for C-rich stars.

In Table 4 we present results of our calculations of p both with and without color corrections of the *IRAS* fluxes (see Table VI.C.6 of the *IRAS* Catalogs and Atlases Explanatory Supplement). Column (3) gives the average values of the flux ratios read from Figures 1*a* and 2. As mentioned above, we could not discern any systematic difference in the flux ratios between 12 and 25 and between 60 and 100 μm for O-rich and C-rich stars so, over these ranges of wavelength, the average value for p, given in columns (4) and (5) of Table 4, applies to all stars independent of C/O. The most reliable number in these columns is the *difference* (0.42) between the mean value of p for O-rich and C-rich stars over the range $25 \leftrightarrow 60$ μm. This is because the difference is largely independent of the values of ξ at 25 and at 60 μm. The least reliable number in the columns is probably the mean value of p (0.9) between 12 and 25 μm because a substantial fraction of the 12 μm flux may be photospheric rather than circumstellar for stars with small mass-loss rates, because of the presence of strong 10 μm silicate emission or absorption which contaminates the 12 μm continuum flux in many O-rich stars, and because a proper calculation of $\xi(12\ \mu m)$ should account for the steepening of $T(r)$ at small r for stars with large mass-loss rates (as described above).

Column (5) in Table 4 suggests an average, color-corrected value for $p(\sim 1.1)$ for carbon stars between 12 and 100 μm. This compares favorably with a previous determination of p extending to 400 μm by Sopka *et al.* (1985), but based on a much smaller sample of stars. Recently, Jura (1986) derived $p = 1.1$ between 12 and 100 μm for a set of carbon stars intermediate in size between the samples investigated by Sopka *et al.* (1985) and by us in the present paper. Because Jura's stars are not especially bright at far-IR wavelengths, his results are likely to be somewhat biased against stars with large values of p between 60 and 100 μm, as he himself notes in his § II.

There are six S-type (C/O $\sim$ 1) stars plotted in Figures 1*a* and 2. From Figure 1*a* we see that, on the average, the emissivity of dust grains in S-type circumstellar envelopes seems more nearly like the emissivity of dust in O-rich rather than C-rich envelopes and that, in addition, the S-type stars do not have especially large amounts of cool dust at large radial distances as judged by the 25 to 12 μm color index.

TABLE 4

MEAN DUST GRAIN EMISSIVITY INDEX [p]

$\lambda_1 \leftrightarrow \lambda_2(\mu m)$ (1)	Type of Star (2)	$\log\left[\frac{\lambda_1 F(\lambda_2)}{\lambda_2 F(\lambda_1)}\right]$ (3)	[p] (uncorr.) (4)	[p] (corr.) (5)
$12 \leftrightarrow 25$......	O-rich and C-rich	−0.7	0.95	0.9
$25 \leftrightarrow 60$......	C-rich	−1.04	1.21	1.12
$25 \leftrightarrow 60$......	O-rich	−1.19	1.63	1.55
$60 \leftrightarrow 100$......	O-rich and C-rich	−0.73	1.5	1.16

There are a few stars in Figures 1 and 2 with unusual far-infrared colors. GX Mon (star 33) has an unusually large 60/25 μm flux ratio for an O-rich star with such a small ratio of $F(25)/F(12)$. R Scl (star 8) and U Cam (star 97) have very large values of $F(60)/F(25)$ for C-rich stars. None of these stars has unusual 100/60 μm flux ratios (Fig. 2). However, AFGL 2513 (star 134) does have a remarkably large 100/60 μm flux ratio. Although it lies in the galactic plane, there are no warning flags in regard to either flux quality or correlation of the *IRAS* source with the point source template at either 60 or 100 μm. Finally, IRC +10216 (star 43) has a remarkably small 100/60 μm flux ratio. We guess that this is due to either a problem with the *IRAS* photometry on such a bright source or perhaps, that some of the 100 μm flux fell outside the *IRAS* detector field of view.

Because there is not a perfect correlation between the location of a star in Figure 1 and its C/O ratio, classification of individual stars based solely on their 12, 25, and 60 μm relative fluxes is not entirely secure. This should be kept in mind when evaluating the reliabilities of the classifications that we suggest in Table 5. Our classifications are given in the middle column of the table. Previous classifications are presented in the right-hand column.

IV. DISCUSSION

In this section we first briefly consider carbon stars with large outflow velocities located near the galactic plane. Then we discuss a number of interesting evolved objects, placing emphasis on their proper classification according to their C/O abundance ratios. Finally, we briefly describe our observations of five *IRAS* sources that are associated with narrow CO or HCN emission lines and are, almost certainly, luminous pre–main-sequence stars.

a) Carbon Stars with Large Outflow Velocities (V_∞)

In Paper II we reported the discovery of a class of carbon stars that has large V_∞ and is located close to the galactic plane. We argued that these stars delineate the most massive carbon-rich objects in our Galaxy. Because of contamination by interstellar CO emission, it was not possible to obtain an accurate measurement of V_∞ for some stars in which we detected circumstellar CO. For others, the contamination is so bad as to preclude totally the possibility of detecting circumstellar CO emission. A conceivable way to circumvent these problems is to observe HCN rather than CO since interstellar HCN lines are usually much weaker than interstellar CO lines, but the same is not necessarily true for HCN and CO from carbon-rich circumstellar envelopes (see § IV*b*).

Included in Table 2 are four stars, AFGL 482, AFGL 67, AFGL 971, and IRC +10401, for which V_∞ as determined from CO emission is uncertain due to blending with interstellar CO lines detected along the line of sight. We detected HCN from AFGL 482, AFGL 67, and IRC +10401 and obtained much improved measurements of V_∞ for the latter two stars. Not only is V_∞ quite large for IRC +10401, but the HCN line, if it originates from a region significantly smaller than our 69″ beam is more intense than the CO line (see Figure 3 and Table 2 of this paper and Table 1 of Paper II). This is the case even though quoted CO and HCN beam-averaged brightness temperatures from IRC +10401 are the same because (1) the HCN data were obtained with a smaller telescope (12 m versus 14 m) and (2) for a given telescope the HPBW is smaller at the CO frequency. The only other example of a source (interstellar or

TABLE 5

LIKELY CLASSIFICATION OF SOME *IRAS* SOURCES

Star	Classification	Remarks	
AFGL 190	C	LRS Classification	O
		Kleinmann et al. (1981)	C?
AFGL 5076	C	LRS Classification	O
IRAS 0331+6058 (AFGL 5098)	C	LRS Classification	O
IRC+60144	C	LRS Classification	C
		RAFGL Classification	O
IRAS 0713+1005	O		
IRAS 0807-3615	C	LRS Classification	O
AFGL 5250	C	LRS Classification	O
IRAS 1705-3753	O		
IRAS 1716-3903	C		
IRAS 1719-3512	C	LRS Classification	O
IRAS 1731-1531	O		
AFGL 5359	O		
AFGL 1992	O	LRS Classification	C
		RAFGL Classification	O
AFGL 5371	?		
AFGL 5369	O		
AFGL 5379	O?		
IRAS 1744-4048	O		
AFGL 5146S	O	LRS Classification	C
IRAS 1751-2526	C?		
AFGL 5416	C?	LRS Classification	O
IRAS 1756-2035	O		
IRAS 1757-3121	O		
IRAS 1758-2201	O		
AFGL 5430	O		
AFGL 5440	C		
AFGL 2067 (FX Ser)	C	LRS Classification	C
		RAFGL Classification	O
IRAS 1808-0338	O		
AFGL 2102	C	LRS Classification	C
		RAFGL Classification	O
AFGL 2143	O		
AFGL 2151	C	LRS Classification	C
		RAFGL Classification	O
IRAS 1834-0839	O		
AFGL 5528	O		
IRAS 1857+0341 (AFGL 2298)	O		
IRAS 1858+0900	O	LRS Classification	C
AFGL 2333	C	LRS Classification	O
AFGL 2343	O		
AFGL 2412 (V1293 Aql)	O	LRS Classification	C
		RAFGL Classification	O
IRAS 1937+0550	O		
IRAS 2002+3910	O		
IRAS 2128+5050	O?		
IRAS 2131+5631	O		
AFGL 3141 (Z Cas)	O	LRS Classification	C
		RAFGL Classification	O

NOTE.—The basis for our classification of many of the stars is described in § IV*b*. If a given star does not appear in § IV*b*, then our classification is based on broad-band *IRAS* fluxes at 12, 25, and 60 μm (see Fig. 1 and § III).

circumstellar) that we are aware of where the HCN line is stronger than the CO line is the carbon star AFGL 2233 (Paper II and Claussen and Ziurys 1985, private communication). It should be possible, with a millimeter λ interferometer, to measure the relative sizes of the HCN and CO emitting regions in IRC +10401 and AFGL 2233 and, hence, to determine the true relative HCN and CO brightness temperatures.

There are three stars in Table 2, AFGL 2023, 2333, and 2513, that have detectable HCN lines but have not yet been detected in CO emission. They are all located in the galactic plane. There may be two different HCN features in the spectrum of AFGL 2023. Obviously, only one can be associated with the star; at least one must be interstellar. Indeed, because the CO spectrum in this direction is exceptionally messy, it is possible that both HCN features are interstellar.

The values of V_∞ given in Table 2 have *not* been corrected for the HCN hyperfine pattern (see, e.g., Olofsson *et al.* 1982). Nonetheless, we believe that these velocities give a reasonable representation of the true circumstellar outflow velocities, as would be measured with a molecule without hyperfine splitting, for the following reason. We have compared HCN and

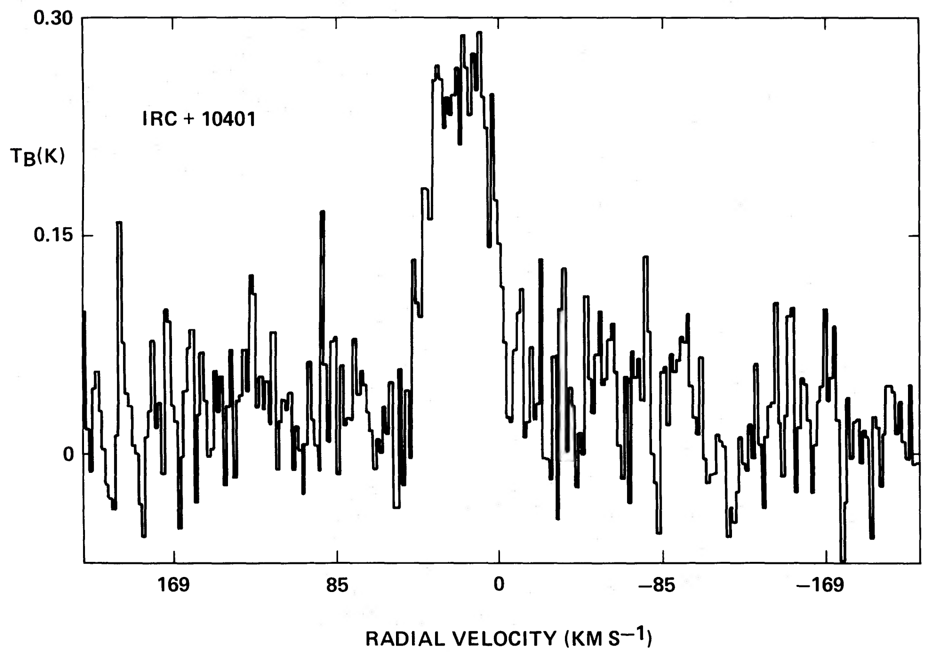

FIG. 3.—Spectrum of HCN emission from IRC +10401. The ordinate is brightness temperature as defined in the text. The abscissa is radial velocity with respect to the local standard of rest referred to a rest frequency of 88.63185 GHz. These data were obtained with the 500 KHz filter bank. With the 1 MHz filter bank, we obtained an equivalent quantity of independent data (not shown here) in the orthogonal sense of polarization. The line parameters given in Table 2 for IRC +10401 are an average of the two data sets.

CO linewidths for nine stars (CIT 6, IRC +60144, V CrB, V Cyg, and AFGL 190, 809, 2233, 2901, and 3068), which should be reasonably representative of cool carbon stars with large mass-loss rates. The quantity V_∞ measured with CO ranges from 6.5 to 34.5 km s^{-1} for the nine stars. The data were taken from Papers I and II, Tables 1 and 2 of the present paper, Sopka *et al.* (1986), and Claussen and Ziurys (1985, private communication). For a given star, V_∞ deduced from HCN usually differs from that derived from the CO profile by less than 2 km s^{-1} and the mean values of V_∞ for the nine stars are virtually the same for HCN and CO.

Therefore, we believe that for the three stars in Table 2 which lie in the galactic plane and for which reliable values of V_∞ do not exist from CO spectra (i.e., IRC +10401, AFGL 2333, AFGL 2513), the value of V_∞ given in Table 2 is a reliable measure of the circumstellar outflow velocity. These V_∞ are consistent with the idea presented in Paper II that carbon stars near the galactic plane tend, on the average, to have relatively large outflow velocities.

Comparison of the central velocities ($V_{\rm LSR}$) of the HCN profiles (Table 2) with $V_{\rm LSR}$ for the same stars as measured with CO emission profiles reveals a striking regularity: the HCN central velocities are systematically redshifted by approximately 3 km s^{-1} with respect to the CO velocities. This effect is already obvious from the high-quality CO and HCN profiles published by Olofsson *et al.* (1982) for IRC +10216 and even earlier for HCN (Zuckerman *et al.* 1976) and CO (Lo and Bechis 1976) line profiles in AFGL 2688. The shift is also present in the high-quality data of Sopka *et al.* (1986).

Presumably, the effect is the result of the HCN hyperfine pattern but, since the splitting of the two strongest components ($F = 2 \rightarrow 1$ and $F = 1 \rightarrow 1$) is only approximately 4 km s^{-1} (see, e.g., Olofsson *et al.* 1982, Fig. 4), it is not at all obvious that the actual measured shift should be so large. Perhaps it is a result of hyperfine population transfer in the HCN, qualitatively similar to the nonlocal transfer effects for OH in an expanding medium described by Morris and Bowers (1980) and by Bujarrabal *et al.* (1980). This idea is discussed in greater detail by Sopka *et al.* (1986).

We further discuss some of the stars in Table 2 in § IV*b* below.

b) *Individual Evolved Stars*

There are six stars that are listed in Table 5 which are *not* discussed below, which do *not* have RAFGL classifications, and for which our classification disagrees with the LRS classification. In each case, we examined the LRS spectrum and found it to be ambiguous. Our classification of these six stars is, therefore, based solely on their location in Figure 1.

The stars that follow are listed in order of increasing right ascension.

AFGL 190.—This star, tentatively identified as carbon-rich by Kleinmann, Gillett, and Joyce (1981), is classified as oxygen-rich in the *IRAS* LRS catalog. We examined the LRS spectrum and find that it is ambiguous, as are the relative broad-band *IRAS* colors (see Fig. 1*a*, star 6). These *IRAS* fluxes peak near 25 μm, which is very unusual if the star is carbon-rich and of a late type. Nonetheless, we believe that AFGL 190 is C-rich because of the relatively intense HCN line that it displays (Table 2).

We have examined HCN and CO data obtained with the 7 m Bell Laboratories (BTL), 12 m NRAO, and 14 m University of Massachusetts antennas, all of which seem to be calibrated reasonably well with respect to each other. For seven cool stars with uncontroversial classifications as C-rich (CIT 6, V CrB, IRC +10401, and AFGL 482, 865, 2233, and 2901), the ratio of T_B, as measured with a given antenna, for CO and for HCN (both $J = 1 \rightarrow 0$) ranges between 0.77 and 5.2. For AFGL 190 we have only a CO $J = 2 \rightarrow 1$ intensity measured with the 12 m telescope (see Paper I). However, for three carbon stars (CIT 6,

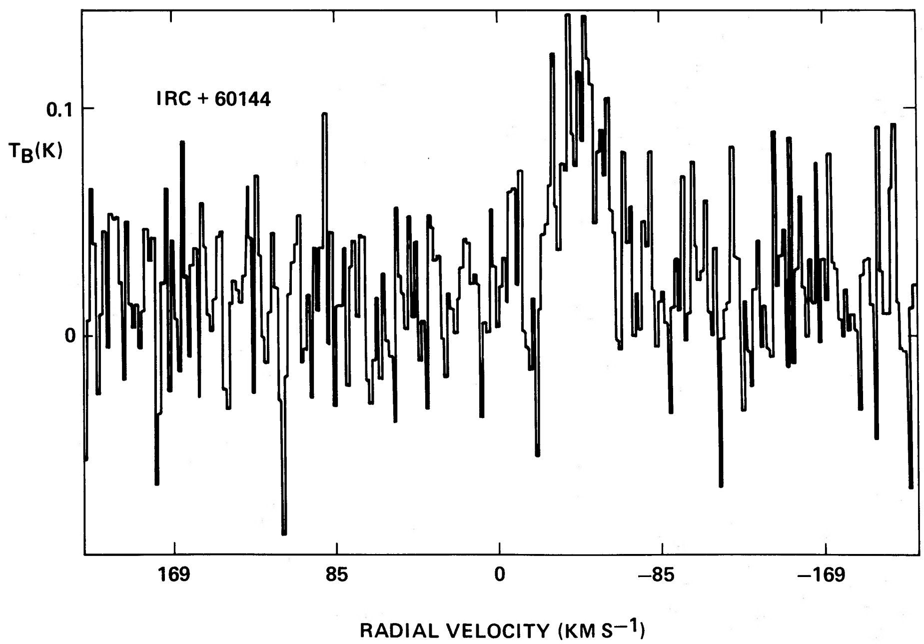

FIG. 4.—Spectrum of HCN emission from IRC +60144. All remarks in the caption to Fig. 3 also apply here.

AFGL 5250, and AFGL 5254) we have measured both the $J = 2 \rightarrow 1$ and $1 \rightarrow 0$ lines on the 12 m telescope (see Paper I and Table 1 of the present paper). The ratios of measured T_B vary between 1.84 and 3.03 with a mean of 2.5. Using this scaling factor, which is very unlikely to be incorrect by as much as even a factor of 2, we deduce that, for AFGL 190, T_B(CO, $J = 1 \rightarrow 0)/T_B$(HCN, $J = 1 \rightarrow 0) = 3.1$. This ratio lies well within the range measured for the seven carbon stars mentioned above.

By way of contrast, only three oxygen-rich stars (NML Tau, IRC +10420, and OH 231.8+4.2) have ever shown detectable HCN lines (Jewell, Schenewerk, and Snyder 1986; Deguchi, Claussen, and Goldsmith 1986). Both IRC +10420 and OH 231.8+4.2 are very unusual stars and we do not consider them further. For NML Tau we estimate that T_B(CO, $J = 1 \rightarrow 0)/T_B$(HCN, $J = 1 \rightarrow 0) = 7.7$. So, even for the O-rich star with the strongest known HCN line, the HCN intensity relative to CO is significantly smaller than it is from AFGL 190.

IRC +60144.—The classification is O-rich in the RAFGL catalog (where the star is mislisted as DO 28489 instead of DO 28389). However, the *IRAS* LRS designation is C-rich and, indeed, there is, apparently, an SiC feature present near 11 μm. The relative broad-band *IRAS* colors are ambiguous (Fig. 1*a*, star 19). We classify the star as C-rich because of the clear SiC feature and because of the strong HCN line that we detected (Table 2 and Fig. 4). In particular, the ratio T_B(CO, $J = 1 \rightarrow 0)/T_B$(HCN, $J = 1 \rightarrow 0) = 4.8$, placing the star in the C-rich range (see discussion of AFGL 190, above).

IRAS 0807−3615.—This star is classified in the *IRAS* Point Source Catalog as O-rich based on its LRS spectrum. However, we examined the LRS spectrum and discern a weak SiC feature near 11 μm implying a C-rich star. The relative broad-band colors (Fig. 1*a*, star 122) also indicate a carbon star.

AFGL 5250.—This star is classified in the *IRAS* Point Source Catalog as O-rich based on its LRS spectrum. We examined the LRS spectrum and found it to be ambiguous. The relative broad-band colors (Fig. 1*a*, star 38) indicate a carbon star. Also, we detected a strong HCN line from AFGL 5250 (see Table 2). Specifically, the ratio T_B(CO, $J = 1 \rightarrow 0)/T_B$(HCN, $J = 1 \rightarrow 0) = 2.9$, placing the star in the C-rich range (see discussion of AFGL 190, above).

V Hya.—"Quasi-thermal," i.e., nonmaser, circumstellar emission lines have characteristically simple shapes which are a function of optical depth and the spatial resolution of the telescope that is used to observe them (e.g., Morris 1985; Olofsson 1985). Very few stars display CO emission profiles that differ noticeably from these characteristic shapes. One noteworthy exception is V Hya which was the first classical carbon star ever detected by radio astronomers (Zuckerman *et al.* 1977). In Figure 5 we display an unpublished spectrum from that reference obtained in 1976 June as well as our new CO spectrum obtained in 1985 June. The narrow (unresolved) spike near the red wing of the latter profile clearly was not present in 1976 June. We believe that the narrow emission feature is real and is associated with V Hya for the following reasons.

The 1985 data are composed of four independent data sets. Two were obtained in orthogonal polarizations on June 4 (UT) and two in orthogonal polarizations on June 5. In all four data sets the narrow spike is present. Because V Hya is located well out of the galactic plane it is very unlikely that this spike could be an interstellar, rather than circumstellar, feature, especially in view of the fact that it was not present in 1976 June. Nonetheless, to be certain, we observed on 1985 June 6 at positions 2′ north and 2′ south of V Hya. The entire CO line disappeared at both positions.

In view of the above, we believe that the spike observed in 1985 June is probably the first CO maser ever seen in any interstellar or circumstellar source. Lo and Bechis (1977) reported time variations in CO emission from Mira, but the variable feature was fairly broad and might represent the quasi-thermal response of the entire circumstellar envelope to

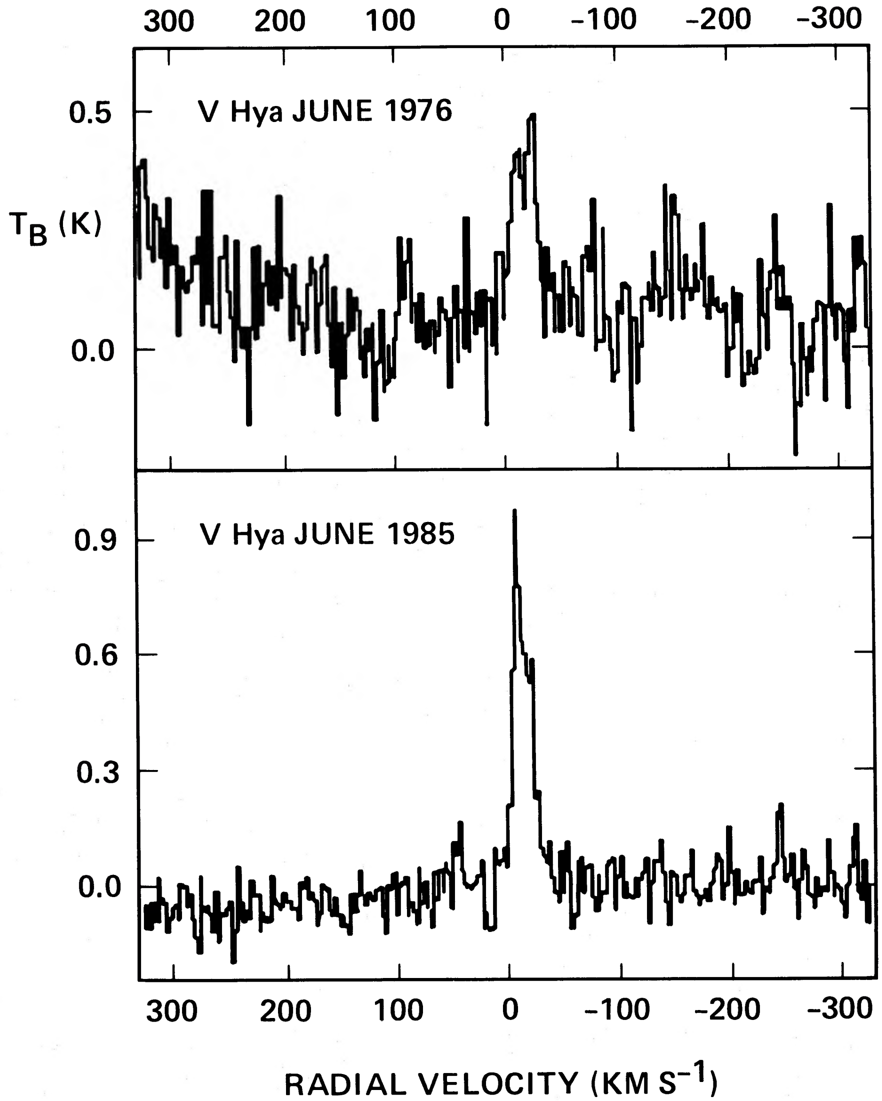

FIG. 5.—Spectra of CO emission from V Hya obtained nine yr apart with 1 MHz filter banks. The ordinate and abscissa are the same as in Fig. 3 but referred to a rest frequency of 115.2712 GHz. See § IV*b* for a detailed discussion of these spectra.

changes in the bolometric luminosity of Mira. (The CO is excited by near-infrared radiation from the star [Morris 1980].)

RT Vir.—Knapp and Morris (1985) reported a tentative (uncertain) detection of the CO $J = 1 \rightarrow 0$ line which we confirm (Table 1).

NGC 6302.—This unusual nitrogen- and oxygen-rich planetary nebula is, possibly, the only evolved stellar object from which the 21 cm hydrogen line has been detected (Rodriguez *et al.* 1985). The 21 cm absorption velocity measured with the VLA is -40 km s^{-1}, which they interpret as due to an expanding shell of neutral hydrogen seen in absorption against the 21 cm continuum source produced by the ionized gas in NGC 6302 which itself has a radial velocity of -31 km s^{-1}. One would expect that CO emission from NGC 6302 would be centered near -31 km s^{-1}, yet we detected CO emission (Fig. 6) near -46 km s^{-1}. Because of this peculiar velocity and the fact that CO has been clearly detected to date from only two other bona fide planetaries (NGC 7027 and NGC 2346), perhaps the CO emission is not associated with NGC 6302 in spite of the fact that the shape of the line profile appears definitely circumstellar and not interstellar. Recently, Terzian (1985) reported OH observations of NGC 6302 obtained with the VLA. The OH profile displays a feature with a peak near -40 km s^{-1} that also has a weaker shoulder extending to -50 km s^{-1}.

AFGL 1992.—This star is classified in the RAFGL catalog as O-rich but in the *IRAS* Point Source Catalog as C-rich based on an apparent SiC feature in its LRS spectrum. We examined the LRS spectrum and find this identification of SiC to be plausible but not entirely convincing. However, the 12, 25, and 60 μm fluxes clearly imply that AFGL is O-rich and we classify it thus.

AFGL 5379.—This is a very red, remarkably bright *IRAS* source but with no LRS classification. The $J = 2 \rightarrow 1$ CO line is of only modest intensity (Table 1), and we were unable to detect the $J = 1 \rightarrow 0$ transition in 1985 June ($T_B < 0.3$ K). The location of AFGL 5379 in Figure 1*b* suggests that it is probably O-rich.

FX Ser (*AFGL 2067*).—The classification is O-rich in the

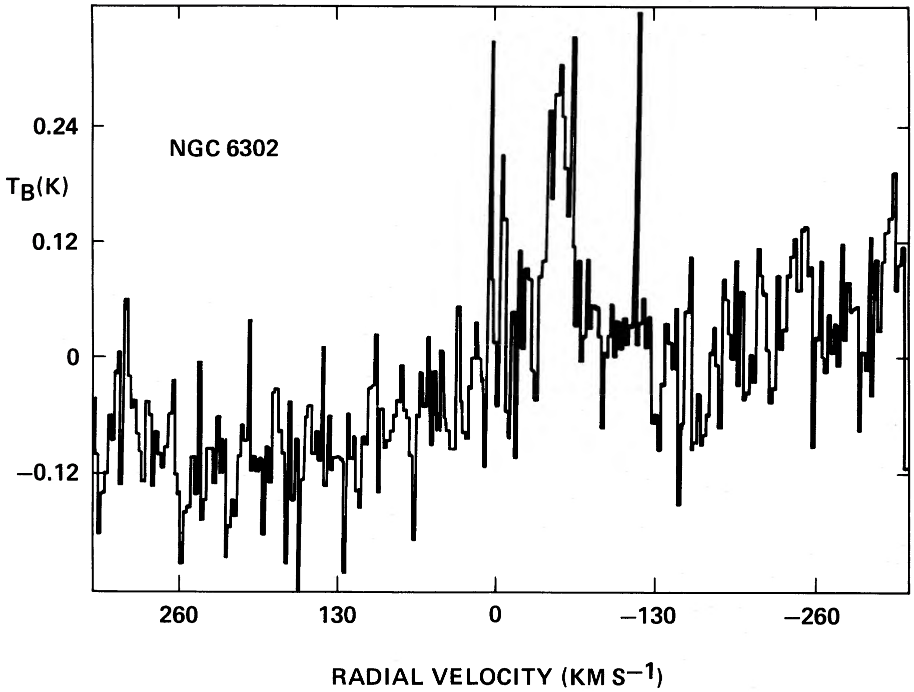

FIG. 6.—Spectrum of CO emission toward the planetary nebula NGC 6302 obtained with the 1 MHz filter banks. The ordinate and abscissa are the same as in Fig. 3 but referred to a rest frequency of 115.2712 GHz.

RAFGL catalog. However, the *IRAS* LRS designation is C-rich and indeed there is, apparently, an SiC feature present near 11 μm. The relative 12, 25, and 60 μm fluxes also indicate a C-rich star, so we classify FX Ser as such.

AFGL 2102.—This star is classified as O-rich in the RAFGL catalog but as C-rich in the *IRAS* Point Source Catalog based on its LRS spectrum. We examined the LRS spectrum and found it to be ambiguous. We classify AFGL 2102 as C-rich based on its relative 12, 25, and 60 μm fluxes.

AFGL 2151.—This star is classified as O-rich in the RAFGL catalog but as C-rich in the *IRAS* Point Source Catalog based on the presence of an SiC feature in the LRS spectrum. We examined the LRS spectrum and found the SiC feature to be convincing. For this reason and because of the relative 12, 25, and 60 μm fluxes, we classify AFGL 2151 as C-rich.

AFGL 2333.—This star is classified in the *IRAS* Point Source Catalog as O-rich based on its LRS spectrum. We examined the LRS spectrum and suspect that a weak SiC feature is present. The relative 12, 25, and 60 μm fluxes also indicate a C-rich star (Fig. 1*a*, star 135). Finally, in Table 2, the star displays a relatively intense HCN feature. (CO has not yet been detected.) Therefore, there can be little doubt that AFGL 2333 is C-rich.

AFGL 2343.—Of the approximately 130 stars with known CO emission, AFGL 2343 has the largest radial velocity with respect to the local standard of rest (Fig. 7, Table 1). Its CO outflow velocity, V_∞ is also large, ~ 34 km s^{-1}, suggestive of a star of supergiant class luminosity. The *IRAS* colors are remarkably red, yet the source is associated with a G-type star. There are many such associations in the *IRAS* Point Source Catalog (Odenwald 1985), but AFGL 2343 must be about the coldest one. If the large radial velocity is due to differential galactic rotation, then AFGL 2343 may be located approximately 6 kpc[3] from Earth and the *IRAS* fluxes would be consistent with a supergiant class luminosity. However, the star is approximately 5° out of the galactic plane, i.e., approximately 500 pc at a distance of 6 kpc. This is a very large displacement from the plane for a supergiant, suggesting that AFGL 2343 may once have been a runaway O-type star (in which case the 6 kpc distance, estimated kinematically, may not be reliable). The star is neither an H_2O maser (Zuckerman and Lo 1986) nor an HCN source (Claussen 1985, private communication).

AFGL 2412.—The classification is O-rich in the RAFGL catalog but C-rich in the *IRAS* Point Source Catalog. Based on the *IRAS* LRS spectrum, which we examined, we classify the star as O-rich in agreement with the RAFGL.

Z Cas (*AFGL 3141*).—The classification is O-rich in the RAFGL catalog but C-rich in the *IRAS* Point Source Catalog based on the LRS spectrum. We examined the LRS spectrum and found it ambiguous. The relative 12, 25, and 60 μm fluxes imply that Z Cas is O-rich in agreement with the RAFGL classification.

c) *Young Stars with Previously Unknown Classifications*

Table 3 lists CO data for four IR sources and HCN data for one (AFGL 5124). In each case a strong, narrow emission line is present. Using the measured radial velocities (V_{LSR}), we estimated rough kinematic distances (D) to the IR sources assuming that they are at the same distance as the CO or HCN. Then we assumed that most of the stellar energy is emitted between 12 and 100 μm and calculated the bolometric luminosities (L_*) given in column (7) of the table. These should

[3] Kinematic distances quoted in this paper for all stars that lie inside the solar circle (at 8.2 kpc) are based on the rotation curve given by Kerr and Westerhout (1965). Outside of 8.2 kpc, we assume a flat rotation curve.

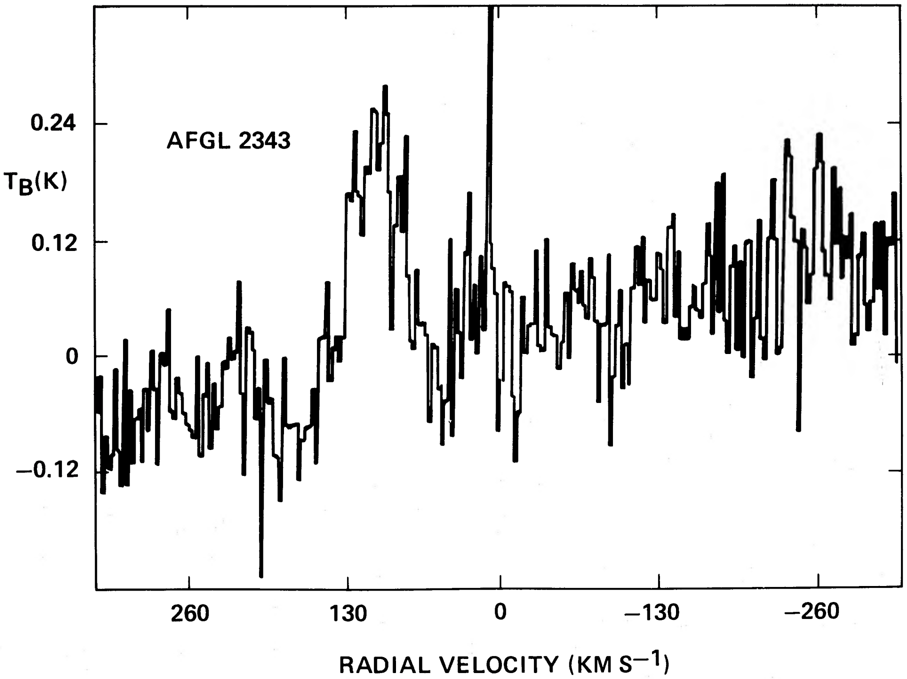

FIG. 7.—Spectrum of CO emission from AFGL 2343 obtained with the 1 MHz filter banks. The ordinate and abscissa are the same as in Fig. 3 but referred to a rest frequency of 115.2712 GHz. The narrow spike near 0 km s^{-1} is real CO emission, presumably local and interstellar, since it was also present 2′ north of AFGL 2343.

be accurate to within a factor of order 2 and indicate that the IR sources are, typically, early B-type stars.

As we discuss below, the physical association of a few of the IR sources with the CO emission is ambiguous because of the large spatial extent of the latter. However, because the far-IR fluxes peak at a wavelength longer than 60 μm, we are reasonably confident that the IR sources are pre– rather than post–main-sequence objects. That is, based on experience gained in carrying out the CO survey reported here, in Papers I and II and in other, as yet unpublished, observations, we can make the following remark concerning pre– and post–main sequence stars. With only a few exceptions, sources with *IRAS* fluxes which peak at a wavelength shorter (longer) than 60 μm are post–main (pre–main)-sequence stars. When we wrote Paper II, we had insufficient experience to recognize either this far-IR regularity or the ambiguities associated with mapping CO emission toward stars located near the galactic plane. Therefore, we now realize that, in Paper II, we too hastily classified AFGL 5497 as a pre–main-sequence star based on its unusual LRS classification and a very inadequate CO map. Because its flux peaks near 25 μm, AFGL 5497 is undoubtedly a post–main-sequence star and the narrow CO line that we observed along the line of sight is unlikely to be associated with it.

A few remarks on the five stars listed in Table 3 follow.

AFGL 5124.—The HCN line is sufficiently narrow that the hyperfine pattern is clearly visible in the spectrum obtained with the 500 kHz filters. A five-point map (center-east-west-north-south) with 2′ offsets indicated that the HCN emission is quite localized and peaks at or very near the *IRAS* position.

AFGL 5206.—The CO line is very narrow, essentially unresolved in the 1 MHz filters. A five-point map with 2′ offsets indicated that the emission is localized near the *IRAS* declination but is, apparently, quite extended in the east-west direction. Indeed, because of the large extent in this direction, we cannot be really certain that the CO emission is associated with the *IRAS* source.

AFGL 5502.—The very strong CO line is very narrow, essentially unresolved in the 1 MHz filters. A five-point map with 2′ offsets indicated that the emission is localized and peaks near the *IRAS* position (perhaps slightly to the north of it).

IRAS 2155+5907.—The CO line is resolved with 1 MHz filters at the *IRAS* position. A five-point map with 2′ offsets indicates that the emission center is localized near the *IRAS* right ascension but is clearly displaced to the south of the *IRAS* declination. Indeed, at the 2′ south offset, the peak T_B was roughly equal to that measured at the *IRAS* position. However, since the line at the south position was very narrow (unresolved) the "equivalent width" of the emission is larger at the *IRAS* position. If the kinematic distance of 10 kpc is correct, then the north-south linear extent of the CO emission is quite large.

IRAS 2214+5206.—The CO line is just barely resolved with the 1 MHz filters at the *IRAS* position. A five-point map with 2′ offsets indicated that the emission is quite extensive. In right ascension, the emission apparently peaks slightly to the east of the *IRAS* position. In declination, the peak T_B at the south offset was roughly equal to that at the *IRAS* position and T_B at the north offset was about one-half as large. Because of this large north-south extent, we cannot be really certain that the CO emission is associated with the *IRAS* source.

V. SUMMARY AND CONCLUSIONS

This paper is the third in a series on mass outflow from red-giant stars. Our primary goal when we began this research was to deduce the relative amounts of mass returned to the interstellar medium by the various types of luminous, evolved stars; Paper I treated this problem in a preliminary, semiquantitative manner. In Paper II, which was concerned, at most, only indirectly with the problem of mass loss, we identified a class of carbon stars that has small galactic latitudes but large circumstellar outflow velocities, V_{∞}, and argued that these stars must be among the most massive carbon-rich objects in our Galaxy. The present paper is related, again only peripherally, to the problem of mass loss. Here we have deduced stellar classifications and some characteristics of circumstellar dust grains that will be useful in future analysis of mass loss from evolved stars. At this point in time, we have detected CO emission ($J = 1 \rightarrow 0$ or $J = 2 \rightarrow 1$) from approximately 80 evolved stars in addition to the approximately 50 that were known previously. We expect, in future observations, to add perhaps another 20 stars to the total and to analyze, quantitatively, the mass-loss rate in gas from these 150 stars. We are modeling also the far-infrared spectrum of these same stars and deducing loss rates in dust grains (Sopka, Dyck, and Zuckerman 1986). The principal results of the present paper follow.

1. We have constructed far-infrared color-color diagrams (Figs. 1 and 2) for over 100 of the brightest evolved stars in the *IRAS* Point Source Catalog. From these diagrams we deduce average values of the dust grain emissivity index, p, between 12 and 100 μm. Grains in C-rich and O-rich environments have similar values of p between 12 and 25 μm and between 60 and 100 μm, but between 25 and 60 μm p is larger by approximately 0.4 for the O-rich stars.

2. Dust grains in envelopes around S-type stars seem to have 25 to 60 μm emissivities more nearly like grains in O-rich rather than C-rich environments.

3. There are a few stars (e.g., GX Mon, R Scl, and AFGL 2513) that appear to have unusual far-infrared colors. If the measured *IRAS* fluxes are indeed correct, then these stars must have either unusual mass-loss histories or else unusual dust grains.

4. We detected HCN emission from 11 stars, including two, or perhaps three, that have not been detected yet in CO emission. These three are located in the galactic plane. The HCN data support the idea, presented in Paper II, that C-rich stars with large outflow velocities are preferentially found at small galactic latitudes.

5. The HCN $J = 1 \rightarrow 0$ lines from IRC +10401 and AFGL 2233 are more intense than the CO $J = 1 \rightarrow 0$ lines from the same stars, suggesting different excitation mechanisms for CO and for HCN. Interferometric measurements should clarify the situation in the future.

6. HCN survey data summarized in Table 2 and, also, in Sopka *et al.* (1986) indicate that there is a systematic red shift, approximately 3 km s^{-1}, of the central velocity of the HCN profile with respect to the CO profile in a given star. Since this shift is larger than expected from a naive examination of the HCN hyperfine splitting, a careful analysis should be carried out of the transfer of radiation in an expanding envelope for a molecule with hyperfine structure.

7. We have classified and reclassified various stars in the *IRAS* Point Source Catalog. Our classifications (Table 5) are based on microwave spectral data, location in the color-color plots (Figs. 1 and 2), and an examination of *IRAS* low-resolution spectrometer (LRS) data.

8. Among the 15 stars that we have detected for the first time in CO emission (Table 1) are included AFGL 2343, a star with an unusually large radial velocity that may be a runaway late-type supergiant, and NGC 6302, an unusual planetary nebula. Because the CO radial velocity does not agree with the radial velocity of NGC 6302, interpretation of the various data on this object is not yet clear. In particular, the CO line may be interstellar.

9. V Hya, a classical carbon star, displayed in 1985 June a narrow CO emission feature in addition to the standard broad stellar-like CO line (Fig. 5). The narrow feature may be the first CO maser observed in a circumstellar or interstellar environment.

10. We detected intense narrow CO emission toward four *IRAS* sources and similar HCN emission toward one additional *IRAS* source. Limited mapping data clearly established the physical association of the microwave emission and the *IRAS* source in two of these five cases but, in the other three, the CO emission was sufficiently extended that the association is not yet certain. Assuming that the CO or HCN emission is, in fact, excited by the far-infrared sources, then one can deduce kinematic distances and minimum luminosities for the *IRAS* sources which, typically, correspond to early B-type stars.

We are grateful to Dr. R. J. Sopka for assisting with the calculations of the ξ integral. Drs. N. J. Evans and S. Beckwidth very kindly obtained CO $J = 2 \rightarrow 1$ data for AFGL 5379 for us. Dr. P. Wannier graciously helped us overcome some rough spots in the utilization of his COMB programs. Ms. Zdenka Plavec and Ms. Laurie Morgan kindly helped modify a 12 m data tape for use with COMB. We are grateful to Mr. Robert L. O'Daniel for expeditiously typing and editing the manuscript and to Dr. M. Morris for comments. Mr. D. W. Kim assisted us at the 12 m telescope and with the preparation of Figure 1. This research was supported in part by NSF grant AST 82-08793 to the University of Hawaii and grant AST 83-18342 to UCLA.

REFERENCES

Bujarrabal, V., Guibert, J., Nguyen-Q-Rieu, and Omont, A. 1980, *Astr. Ap.*, **84**, 311.
Deguchi, S., Claussen, M. J., and Goldsmith, P. 1986, *Ap. J.*, **303**, 810.
Erickson, K., *et al.* 1986, *Astr. Ap.*, submitted.
Forrest, W. J., Houck, J. R., and McCarthy, J. F. 1981, *Ap. J.*, **248**, 195.
Gehrz, R. D., and Hackwell, J. A. 1976, *Ap. J. (Letters)*, **206**, L161.
Goebel, J. H., and Moseley, S. H. 1985, *Ap. J. (Letters)*, **290**, L35.
Hacking, P., *et al.* 1985, *Pub. A.S.P.*, **97**, 616.
Jewell, P. R., Schenewerk, M. S., and Snyder, L. E. 1986, preprint.
Joyce, R. R., Capps, R. W., Gillett, F. C., Grasdalen, G., Kleinmann, S. G., and Sargent, D. G. 1977, *Ap. J. (Letters)*, **213**, L125.
Jura, M. 1986, *Ap. J.*, **303**, 327.
Kerr, F. J., and Westerhout, G. 1965, in *Galactic Structure*, ed. A. Blaauw and M. Schmidt (Chicago: University of Chicago Press), p. 167.
Kleinmann, S. G., Gillett, F. C., and Joyce, R. R. 1981, *Ann. Rev. Astr. Ap.*, **19**, 411.
Kleinmann, S. G., and Payne-Gaposchkin, C. 1979, *Earth Extraterrestrial Sci.*, **3**, 161.
Knapp, G. R., and Morris, M. 1985, *Ap. J.*, **292**, 640.
Lebofsky, M. J., Sargent, D. L., Kleinmann, S. G., and Rieke, G. H. 1978, *Ap. J.*, **219**, 487.
Lo, K. Y., and Bechis, K. 1976, *Ap. J. (Letters)*, **205**, L21.
———. 1977, *Ap. J. (Letters)*, **218**, L27.
Low, F. J., Kurtz, R. F., Vrba, F. J., and Rieke, G. H. 1976, *Ap. J. (Letters)*, **206**, L153.
Morris, M. 1980, *Ap. J.*, **236**, 823.
———. 1985, in *Mass Loss from Red Giants*, ed. M. Morris and B. Zuckerman (Dordrecht: Reidel), p. 129.

Morris, M., and Bowers, P. F. 1980, *A.J.*, **85**, 724.
Odenwald, S. F. 1985, in *First International IRAS Symposium: Light on Dark Matter*, ed. F. Israel (Dordrecht: Reidel).
Olofsson, H. 1985, in *Workshop on Submillimeter Astronomy*, ed. P. A. Shaver (Garching: European Southern Observatory).
Olofsson, H., Johansson, L. E. B., Hjalmarson, A., and Nguyen-Q-Rieu. 1982, *Astr. Ap.*, **107**, 128.
Price, S. D., and Murdock, T. L. 1983, *The Revised AFGL Infrared Sky Survey Catalog*, AFGL-TR-83-0161.
Rodriguez, L. F., *et al.* 1985, *M.N.R.A.S.*, **215**, 353.
Sopka, R. J., Dyck, H. M., and Zuckerman, B. 1986, in preparation.
Sopka, R. J., *et al.* 1985, *Ap. J.*, **294**, 242.
Sopka, R. J., Olofsson, H., Johansson, L. E. B., Nguyen-Q-Rieu, and Zuckerman, B. 1986, in preparation.
Terzian, Y. 1985, Paper presented to Commission 34 at the XIX IAU General Assembly, Delhi, India.
Zuckerman, B., and Dyck, H. M. 1986, *Ap. J.*, **304**, 394 (Paper I).
Zuckerman, B., Dyck, H. M., and Claussen, M. J. 1986, *Ap. J.*, **304**, 401 (Paper II).
Zuckerman, B., Gilra, D., Turner, B. E., Morris, M., and Palmer, P. 1976, *Ap. J. (Letters)*, **205**, L15.
Zuckerman, B., and Lo, K. Y. 1986, *Astr. Ap.*, in press.
Zuckerman, B., Palmer, P., Morris, M., Turner, B. E., Gilra, D. P., Bowers, P. F., and Gilmore, W. 1977, *Ap. J. (Letters)*, **211**, L97.

Note added in proof.—I. R. Little-Marenin (*Ap. J.* (*Letters*), **307**, L15, [1986]) has reported three carbon stars with strong 10 μm silicate emission features in their LRS spectra! We have checked the location of these stars in our color-color plot (Fig. 1). They all lie clearly in the region that contains oxygen-rich stars. Indeed, V778 Cyg has an especially small ratio $F(60)/F(25)$. This result confirms the oxygen-rich nature of the dust grains in the three stars. The 25 and 60 μm fluxes originate from cooler grains that are farther from the stars than the grains that are responsible for the silicate features. Therefore, the grains that carry the observed 10 μm emission features were not produced in a very short-lived unusual event in the history of each of the three stars.

H. M. Dyck: Department of Physics and Astronomy, University Sta. Box 3905, University of Wyoming, Laramie, WY 82071

B. Zuckerman: Astronomy Department, UCLA, Los Angeles, CA 90024